Clays and Clay Minerals, Vol. 47, No. 2, 192–200, 1999.

MONTE CARLO SIMULATION OF THE TOTAL RADIAL DISTRIBUTION FUNCTION FOR INTERLAYER WATER IN SODIUM AND POTASSIUM MONTMORILLONITES

GARRISON SPOSITO, SUNG-HO PARK, AND REBECCA SUTTON

Earth Sciences Division, Mail Stop 90-1116, Lawrence Berkeley National Laboratory, Berkeley, California 94720-3110

Abstract—Monte Carlo simulations based on tested water-water, cation-water, and water-clay potential functions were applied to calculate radial distribution functions for O-O, O-H and H-H spatial correlations in the interlayer region of the two-layer hydrates of Na- and K-montmorillonite. The simulated radial distribution functions then were used to compute the total radial distribution function for interlayer water, a physical quantity that can be determined experimentally by H/D isotopic-difference neutron diffraction. The simulated total radial distribution functions were compared with that for bulk liquid water, and with a total radial distribution function determined experimentally for the two-layer hydrate of Na-montmorillonite by Powell *et al.* (1997). This comparison suggested that water molecules in the two-layer hydrate of montmorillonite have nearest-neighbor configurations which differ significantly from the tetrahedral ordering of nearest neighbors that characterizes bulk liquid water.

Key Words—Adsorbed Water, Montmorillonite, Neutron Diffraction, Water.

INTRODUCTION

Neutron diffraction studies of interlayer water in hydrated 2 : 1 clay minerals based on isotopic-difference techniques have provided valuable insight as to the molecular structure of the electrical double layer on the surfaces of these minerals (Hawkins and Egelstaff, 1980; Skipper *et al.*, 1991, 1994, 1995c). Powell *et al.* (1997) recently improved on the pioneering work of Hawkins and Egelstaff (1980) with a H/D isotopic-difference investigation of water in the two-layer hydrate of Na-Wyoming montmorillonite. Their principal experimental result was a first-order-difference total radial distribution function for adsorbed D_2O molecules, obtained under conditions in which no D replacement of clay mineral H atoms occurred. This experimental distribution function was compared to a hypothetical model distribution function based on available neutron diffraction data for bulk liquid water (Soper and Phillips, 1986). Powell *et al.* (1997) noted significant deviations between the interlayer total radial distribution function for adsorbed water and their model over intermolecular distances between 1.5–3 Å, leading them to conclude that the nearest-neighbor coordination of adsorbed water molecules in the two-layer hydrate differed significantly from the well known local tetrahedral coordination that exists among water molecules in the bulk liquid (Beveridge *et al.*, 1983; Kusalik and Svishchev, 1994).

This same conclusion was obtained in a variety of recent Monte Carlo simulation studies of the molecular structure of interlayer water in the two-layer hydrate of Na-Wyoming montmorillonite (Chang *et al.*, 1995; Boek *et al.*, 1995a, 1995b; Karaborni *et al.*, 1996). Chang *et al.* (1995) and Boek *et al.* (1995b) both noted that water molecules in this hydrate were organized primarily to accommodate the solvation requirements of Na^+ counterions bound in surface complexes on the basal planes of the clay mineral. Karaborni *et al.* (1996) commented that water protons were also attracted to surface oxygen ions near tetrahedral charge sites on the clay mineral to form hydrogen bonds, whereas water oxygens were attracted to the protons in structural OH groups at the bottom of the ditrigonal cavities in the clay mineral surface. This competition for adsorbed water molecules by counterions, surface oxygen ions, and OH protons in the clay mineral structure would tend to disrupt the local tetrahedral coordination among water molecules that characterizes the bulk liquid.

Chang *et al.* (1995) calculated radial distribution functions representing O-O and O-H spatial correlations in interlayer water on Na-montmorillonite as part of the interpretation of their Monte Carlo simulation output. These two radial distribution functions, along with that for H-H spatial correlations, are in fact the principal contributors to the experimental total radial distribution function reported by Powell *et al.* (1997). The present study was undertaken, therefore, to perform Monte Carlo simulations of the total radial distribution function for interlayer water in the two-layer hydrate of Na-montmorillonite. The total radial distribution function for interlayer water in K-montmorillonite also was simulated to evaluate more precisely the effects of cation solvation, which is much weaker for K^+ than it is for Na^+ (Ohtaki and Radnai, 1993). To examine the inherent quality of our simulations of interlayer water structure in more detail, bulk liquid O-O, O-H, and H-H radial distribution functions based on the model for water molecule interactions used in our Monte Carlo simulations were compared to recent

experimental O-O, O-H, and H-H radial distribution functions for liquid water based on H/D isotopic-difference neutron diffraction data (Soper *et al.*, 1997).

TOTAL RADIAL DISTRIBUTION FUNCTION

The measured intensity of neutron diffraction by an aqueous system, after instrumental calibration and corrections for unwanted scattering events, yields information about the spatial distribution of atoms in the system through the relationship (Enderby and Neilson, 1981):

$$F_T(k) = 4\pi\frac{N}{V}\int_0^R G(r)\frac{\sin kr}{kr}r^2\,dr \qquad (1)$$

where $NF_T(k)$ is the intensity of neutron diffraction at wavenumber $k > 0$, N is the total number of atoms in a system with volume $V \equiv 4\pi R^3/3$ and

$$G(r) = \sum_\alpha \sum_\beta c_\alpha c_\beta b_\alpha b_\beta [g_{\alpha\beta}(r) - 1] \qquad (2)$$

is termed the total radial distribution function (Soper, personal communication, 1998), whose Fourier transform in Equation (1) is proportional to $F_T(k)$. The experimental context for Equation (1), isotopic-difference neutron diffraction, is reviewed by Skipper *et al.* (1991, 1994) for applications to hydrated 2:1 clay minerals, and by Enderby (1983), Neilson and Enderby (1989), Skipper and Nielsen (1989) and Ohtaki and Radnai (1993) for applications to aqueous solutions.

The total radial distribution function $G(r)$ provides a relative measure of the likelihood of coherent neutron scattering at wavenumber k by atoms located at a distance r from some atom placed at the origin of coordinates (Enderby and Neilson, 1981). Equation (2) shows that $G(r)$ depends on the atomic fraction of the scattering atom c_β, on its coherent scattering length b_β and on the radial distribution function $g_{\alpha\beta}(r)$, which is defined implicitly by the equation (Enderby and Neilson, 1981):

$$dn_{\alpha\beta} = 4\pi\frac{N_\beta}{V}g_{\alpha\beta}(r)r^2\,dr. \qquad (3)$$

In Equation (3), $dn_{\alpha\beta}$ is the average number of β-species atoms within a spherical shell of radius r and thickness dr enclosing an α-species atom which has been placed at $r = 0$, and N_β is the total number of β atoms in the system of volume V. Thus $g_{\alpha\beta}(r)$ is the relative probability that a β atom resides within dr at a radial distance r from an α atom centered at the origin of coordinates (Allen and Tildesley, 1987). It is normalized such that

$$N_{\alpha\beta}(\rho) = 4\pi\frac{N_\beta}{V}\int_0^\rho g_{\alpha\beta}(r)r^2\,dr \qquad (4)$$

is the number of β atoms around the central α atom within a sphere of radius $\rho \leq R$ (Beveridge *et al.*, 1983). As $r \uparrow R$, $g_{\alpha\beta}(r) \sim 1$ in an isotropic system (where $\uparrow$ means "approaches from below"), signifying a uniform distribution of β atoms around the central α atom, and $G(r)$ in Equation (2) correspondingly goes to zero, indicating no likelihood of coherent neutron scattering by atoms far from that placed at the origin of coordinates.

The physical role played by $G(r)$ in Equation (2) is as a relative probability for finding any β atom that appears non-randomly at a distance r from an α atom placed at the origin, depending on the relative population of each type of atom (c_β or c_α) and on its ability to scatter neutrons coherently (b_β or b_α). Effective contributions to $G(r)$ and, therefore, to neutron diffraction, come from atoms that are abundant, with large coherent scattering lengths, and which have strong spatial correlations with atoms of any of the species considered. In applications to neutron diffraction by the atoms in the interlayer region of a hydrated clay mineral, Equations (1) and (2) implicitly must be averages over spatial correlations that depend on the direction from a central atom, as well as on the intermolecular distance, given the constrained geometry of clay interlayers. Thus, $G(r)$ and its component radial distribution functions are interpreted structurally as angularly-averaged quantities when applied to species in clay interlayers.

METHODS

Total radial distribution functions

Total radial distribution functions were calculated with Equation (2) for interlayer water in the two-layer hydrates of Na- and K-montmorillonite and for bulk liquid water. The coherent scattering lengths tabulated by Skipper *et al.* (1995c) for H (−3.74 fm), D (6.67 fm), and O (5.81 fm) were used in all computations. Atomic fractions for atoms in the montmorillonite hydrates were calculated with the formula:

$$c_\alpha = \frac{\alpha \text{ atoms per unit cell}}{64.75} \qquad (5)$$

α denotes the type of atom (H, O, or O_2 for O in the clay mineral) and denominator represents 40.75 atoms in the unit cell or dehydrated Wyoming montmorillonite ($M_{0.75}[Si_{7.75}Al_{0.25}]$ $(Al_{3.5}Mg_{0.5})O_{20}(OH)_4$; M = Na or K) plus 24 atoms in interlayer water per unit cell of the clay mineral. This latter number is based on eight water molecules per unit cell in the two-layer hydrate, which is equivalent to a gravimetric D_2O content of 0.218 kg kg^{-1} (Na-clay) or 0.214 kg kg^{-1} (K-clay). The atomic fractions used for bulk liquid water were $c_D = 0.6667$ and $c_O = 0.3333$, as follows from the chemical formula of D_2O.

Table 1 lists values of the coefficients $c_\alpha c_\beta b_\alpha b_\beta$ that appear in Equation (2) and were used in the calculation of $G(r)$ for the montmorillonite hydrates or for bulk liquid water. The coefficients pertaining to the two-

https://doi.org/10.1346/CCMN.1999.0470209 Published online by Cambridge University Press

Table 1. Coefficients used to calculate $G(r)$ for the two-layer montmorillonite hydrate or for bulk liquid water (Units of barns, 1 b = 100 fm^2). The symbol O2 refers to clay mineral O atoms.

Two-layer hydrate[1]			
$c_D^2 b_D^2$	$2c_D c_O b_D b_O$	$2c_D c_{O2} b_D b_O$	$2c_D c_H b_D b_H$
0.0272	0.0237	0.0710	−0.0076
$c_O^2 b_O^2$	$2c_O c_{O2} b_O^2$		
0.0052	0.0309		
Bulk liquid water			
$c_D^2 b_D^2$	$2c_D c_O b_D b_O$	$c_O^2 b_O$	
0.1978	0.1722	0.0375	

[1] Strictly speaking, $G(r)$ for the two-layer hydrate should include terms for spatial correlations between D or O in D_2O and the cations in the clay mineral structure. The corresponding coefficients, however, are all smaller in absolute value than the coefficient $2c_D c_H b_D b_H$ above, except for the coefficient $2c_D c_{Si} b_D b_{Si}$ (=0.01637) which multiplies a radial distribution function nearly equal to 1.0 (no spatial correlation), thus giving a negligibly small contribution to $G(r)$.

layer hydrate differ from those used by Powell *et al.* (1997), who set the denominator in Equation (5) equal to 69.25, corresponding to 9.5 water molecules per unit cell instead of 8, thus resulting in different values for the atomic fractions from those used in the present study. This larger number of water molecules per unit cell adopted by Powell *et al.* (1997) appears to be an error, because it corresponds to a gravimetric D_2O content of 0.258 kg kg^{-1} for Na-montmorillonite, whereas an experimentally-measured D_2O content of only 0.205 ± 0.005 kg kg^{-1} was reported by Powell *et al.* (1997), which is equivalent to 7.5 water molecules per unit cell. The coefficients $c_\alpha c_\beta b_\alpha b_\beta$ in Table 1 pertaining to $G(r)$ for bulk liquid water also differ from those used by Powell *et al.* (1997), who elected to include atomic fractions for the clay mineral structural O atoms along with those for water molecule O atoms to calculate a hypothetical model $G(r)$ instead of the true $G(r)$ for the bulk liquid phase.

Two working forms of Equation (2) were used in the computation of $G(r)$ for r in the range 1.5–6.0 Å. For the two-layer hydrates of Na- and K-montmorillonite,

$$G_h(r) = 0.0947 g_{OH}(r) + 0.0361 g_{OO}(r) + 0.0272 g_{HH}(r) - 0.1579 \quad (6)$$

whereas for bulk liquid water,

$$G_w(r) = 0.1722 g_{OH}(r) + 0.0375 g_{OO}(r) + 0.1978 g_{HH}(r) - 0.4075 \quad (7)$$

where the numerical prefactors derive from appropriate combinations of the coefficients in Table 1. The radial distribution functions in Equation (6), which do not distinguish between O and O2, were calculated by Monte Carlo simulation following the phase-space sampling strategy outlined by Chang *et al.* (1997). The radial distribution functions used in Equation (7) were both calculated by Monte Carlo simulation and taken from smoothed experimental results reported recently by Soper *et al.* (1997) in their extensive reanalysis of isotopic-difference neutron diffraction studies of D_2O/H_2O mixtures.

Monte Carlo simulations

Monte Carlo (MC) simulations of interlayer water structure in two-layer montmorillonite hydrates were performed on Cray J90 supercomputers at the National Energy Research Scientific Computing Center using the code MONTE. Skipper *et al.* (1995a, 1995b) have discussed the application of MONTE to simulate interlayer configurations in hydrates of Wyoming montmorillonite. Chang *et al.* (1997) outlined a strategy for obtaining efficient convergence in MC simulations of these hydrates using MONTE and an isothermal-isostress ensemble (T = 300 K, σ_{zz} = 100 *kPa*).

Potential functions based on the MCY model (Matsuoka *et al.*, 1976) were used to represent all relevant interactions: clay-clay, clay-counterion, clay-water, counterion-counterion, counterion-water, and water-water. The mathematical form of the potential functions used was:

$$U(r_{ij}) = \sum_{i=1}^{N} \sum_{j>i}^{N} \left[\frac{q_i q_j}{r_{ij}} - A_{ij} e^{-B_{ij} r_{ij}} + C_{ij} e^{-D_{ij} r_{ij}} \right] \quad (8)$$

where q_i is the effective charge on a site in a water molecule, in an interlayer cation, or in the clay mineral structure, r_{ij} is the intersite separation distance and the parameters A, B, C, and D describe short-range interactions. Values of all parameters in Equation (8) for Na- and K-montmorillonite hydrates were given by Skipper *et al.* (1995a) and Chang *et al.* (1998), respectively. The advantages and limitations of the MCY model for simulating montmorillonite hydrates were discussed in detail by Skipper *et al.* (1995b) and Chang *et al.* (1997).

The simulation cell comprises two clay mineral half-layers sandwiching the interlayer space. The cell holds eight crystallographic unit cells; thus it has an area of 21.12 × 18.28 Å^2. Isomorphic substitutions of Al^{3+} for Si^{4+}, and of Mg^{2+} for Al^{3+}, create two tetrahedral negative-charge sites and four octahedral negative-charge sites in the layer structure which are balanced by monovalent counterions, as indicated by the unit-cell formula given below Equation (5). Sixty-four water molecules, corresponding to a two-layer hydrate of montmorillonite (Bérend *et al.*, 1995), were randomly placed within the interlayer region of the simulation cell. The simulation cell is repeated infinitely in every direction via three-dimensional boundary conditions. A real-space cutoff of 9 Å is employed for all short-range interactions, while a three-dimensional Ewald sum technique is used for calculating long-

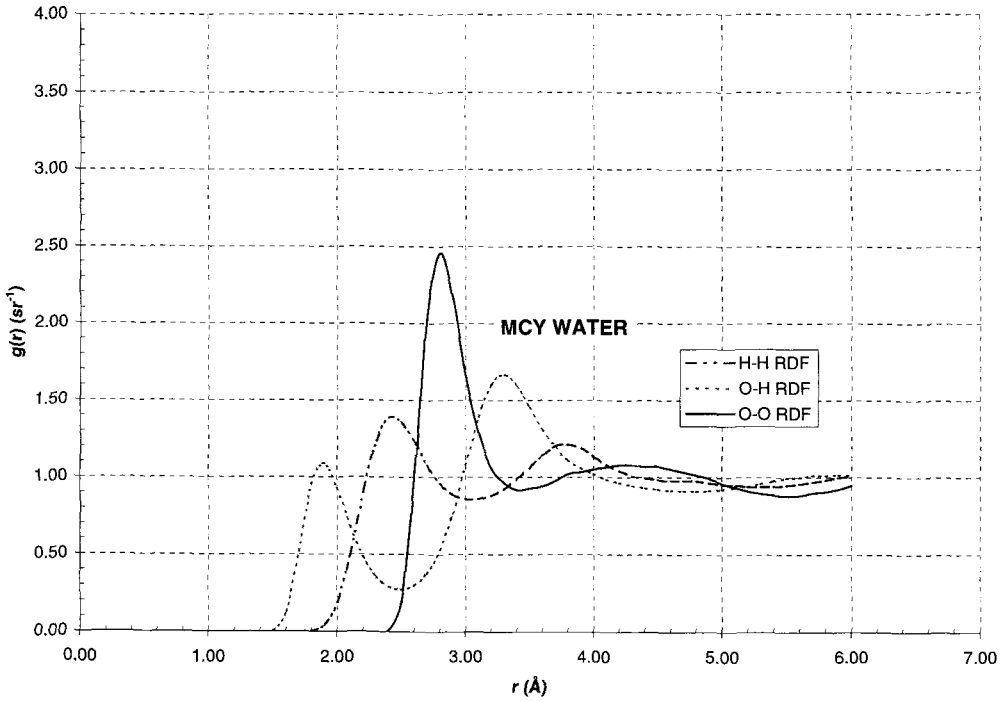

Figure 1. Composite graph of the RDFs representing O-O, O-H, and H-H spatial correlations in MCY water (MC simulation).

range coulomb interactions (Allen and Tildesley, 1987).

Simulation strategies

For simulations of the montmorillonite hydrates, two different initial conditions were employed: (1) all interlayer cations are placed at the midplane between the two clay layers (which is also the central plane of the simulation cell), and (2) four of the interlayer cations are positioned at the midplane over sites of isomorphic substitution in the octahedral sheet whereas the two remaining cations are placed close to the clay mineral surface near sites of isomorphic substitution in the tetrahedral sheet.

In a first optimizing part of the computation, (50,000 steps for Na-montmorillonite or 10,000 steps for K-montmorillonite), only water molecules were permitted to move while the layer spacing (16 Å) and the interlayer cations remained fixed. In the next (50,000 or 10,000) steps, water molecules moved and the clay layer was permitted to move in the z direction (normal to the clay layer). In the next part of the computation (100,000 or 200,000 steps), water molecules, cations, and the clay layer were allowed to move in every direction, with the upper clay layer moved one step in any one direction for approximately every five movements of interlayer water molecules. In the next 1,000,000 steps and for the final part of the computation (500,000 steps), the same conditions as given in the 100,000 (or 200,000)-step computation were applied, with the last 500,000 steps used for data analysis. For all parts of the computation, data were collected for averaging after every 500 steps. Final output included total potential energy, layer spacing (under 100 *kPa* applied normal stress), and radial distribution functions of interlayer water molecules. Simulations begun with the initial condition (2) above always produced the lower and more stable potential energy and layer spacing. Therefore, they were chosen for the final data analysis.

Simulations of bulk liquid water were carried out in an isothermal-isochoric (*NVT*) ensemble using the MCY potential function with a real-space cutoff of 8 Å. A total of 267 water molecules were simulated in an 8000 Å^3 cubic box (corresponding to a fixed density of 0.9976 *Mg* m^{-3}). Simulations with 1.2 to 1.7 million total steps were performed at 300 K. The last 500,000 steps were used for data analysis.

RESULTS AND DISCUSSION

Bulk liquid water

Radial distribution functions (RDFs) for O-O, O-H, and H-H spatial correlations in bulk liquid water are shown in Figures 1 and 2. The RDFs obtained in the present study by MC simulation based on the MCY model appear in Figure 1. The average internal energy of MCY water in our simulation was found to be -8.47 ± 0.07 kcal mol^{-1}, which may be compared to -8.7 ± 0.1 kcal mol^{-1} obtained in a MC simulation using the MCY model by Beveridge *et al.* (1983) and

https://doi.org/10.1346/CCMN.1999.0470209 Published online by Cambridge University Press

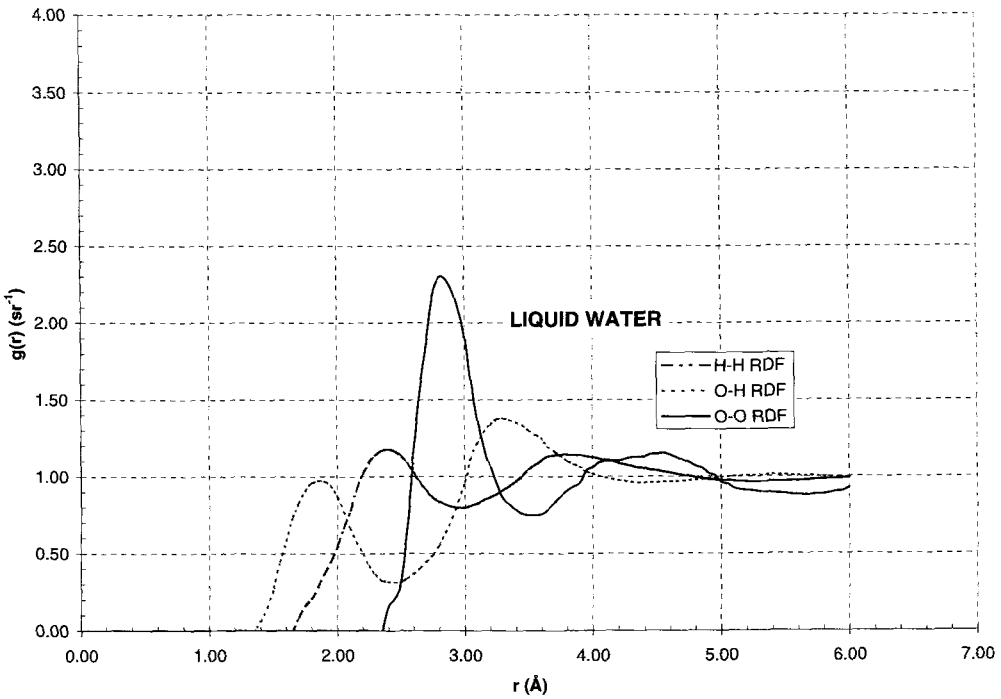

Figure 2. Composite graph of the RDFs representing O-O, O-H, and H-H spatial correlations in liquid water as determined experimentally by Soper *et al.* (1997).

to the experimental value they give, −10 kcal mol^{-1}. Comparison of Figure 1 with Figure 2, which shows RDFs for liquid water based on a recent refinement of neutron diffraction data obtained using the H/D contrast variation method (Soper *et al.*, 1997), indicates that the MCY model, when constrained to the experimental liquid density, reproduces peak positions in the RDFs extremely well, but gives peaks that are somewhat higher than those in the experimental RDFs. The effect of this latter small discrepancy is seen quantitatively in Table 2, which lists intermolecular nearest-neighbor coordination numbers calculated by numerical quadrature according to Equation (4) using the RDFs in Figures 1 and 2. The MCY model predicts N_{OO} and N_{OH} rather well, but overpredicts N_{HH} by ~13%, implying that local spatial ordering as predicted by the MCY model is somewhat different from what actually exists in liquid water (Beveridge *et al.*, 1983; Kusalik and Svishchev, 1994). Nonetheless, Figures 1 and 2, along with the results in Table 2, attest to the essential reliability of the MCY model, at least for predicting RDFs and nearest-neighbor coordination numbers.

Table 2. Intermolecular coordination numbers[1] for bulk liquid water and for adsorbed water in the two-layer hydrates of Na- and K-montmorillonite.

N_{OO}	r_{min}(Å)	N_{OH}	r_{min}(Å)	N_{HH}	r_{min}(Å)
Experimental (Soper *et al.*, 1997)					
5.4	3.50	2.0	2.45	5.3	2.95
MCY water					
5.2	3.40	2.1	2.50	6.0	3.00
Na-montmorillonite hydrate					
9.7	4.00	1.6	2.50	6.1	3.20
K-montmorillonite hydrate					
6.3	3.70	1.4	2.50	4.0	3.10

[1] Intramolecular contributions (2.0 for N_{OH} and 1.0 for N_{HH}) have been subtracted from the value of the integral in Equation (4), with its upper limit set at $\rho = r_{min}$.

Interlayer hydrate water

The RDFs calculated by MC simulation for interlayer water in the two-layer hydrates of Na- and K-montmorillonite are shown in Figures 3 and 4, respectively. The equilibrium layer spacings predicted in the simulation results [15.0 ± 0.1 Å (Na), 15.5 ± 0.2 Å (K)] are in good agreement with the average of the published experimental values for two-layer hydrates of Na- or K-montmorillonite, 15.6 ± 0.5 Å (Posner and Quirk, 1964; Calvet, 1972; Cebula *et al.*, 1980; Zhang and Low, 1989; Fu *et al.*, 1990; Slade *et al.*, 1991; Bérend *et al.*, 1995). The amplitudes of the interlayer water RDFs relative to those for bulk liquid water reflect differences in spatial correlations, simulation cell volume, and atomic composition. The much larger distance to the first minimum of $g_{OO}(r)$ in interlayer water ($r_{min} \approx$ 3.7–4.0 Å) signals an important

https://doi.org/10.1346/CCMN.1999.0470209 Published online by Cambridge University Press

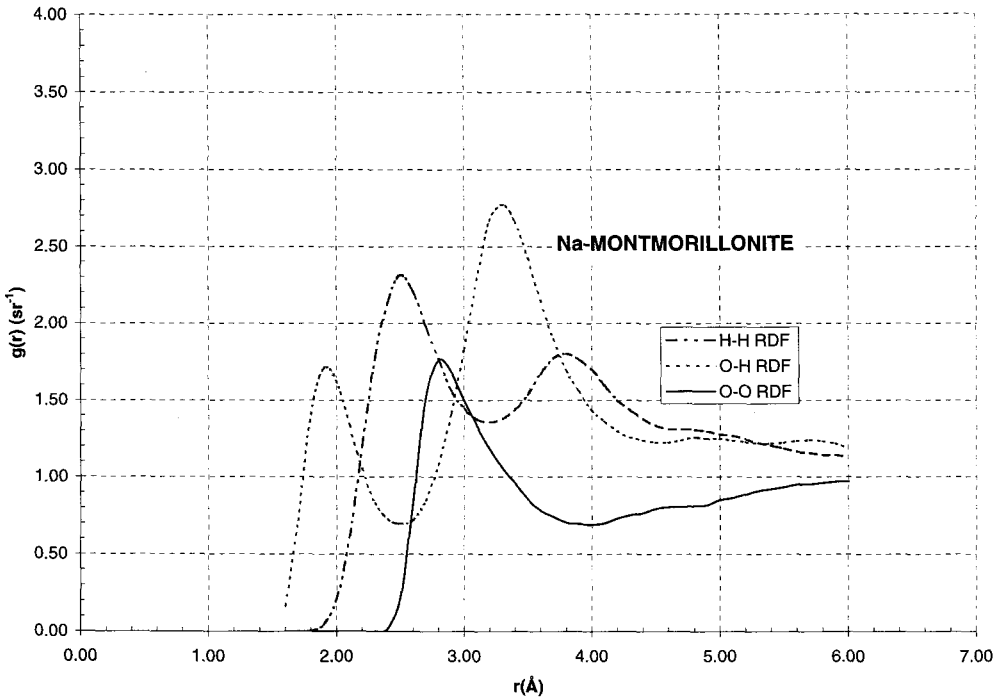

Figure 3. Composite graph of the RDFs representing O-O, O-H, and H-H spatial correlations in interlayer water in the two-layer hydrate of Na-montmorillonite, as calculated by MC simulation.

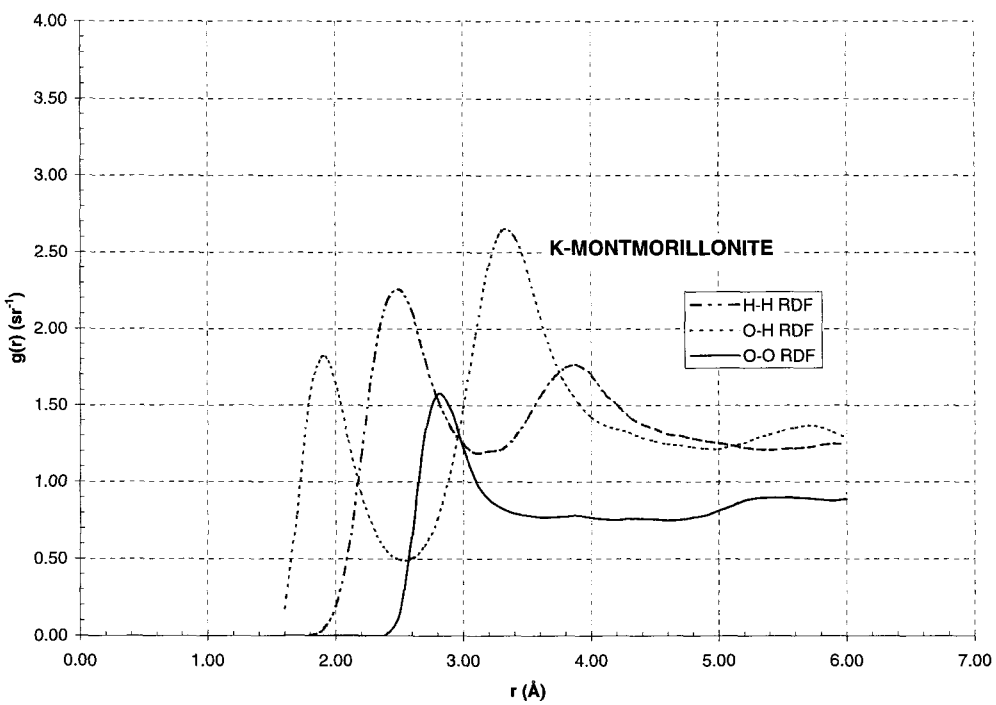

Figure 4. Composite graph of the RDFs representing O-O, O-H, and H-H spatial correlations in interlayer water in the two-layer hydrate of K-montmorillonite, as calculated by MC simulation.

https://doi.org/10.1346/CCMN.1999.0470209 Published online by Cambridge University Press

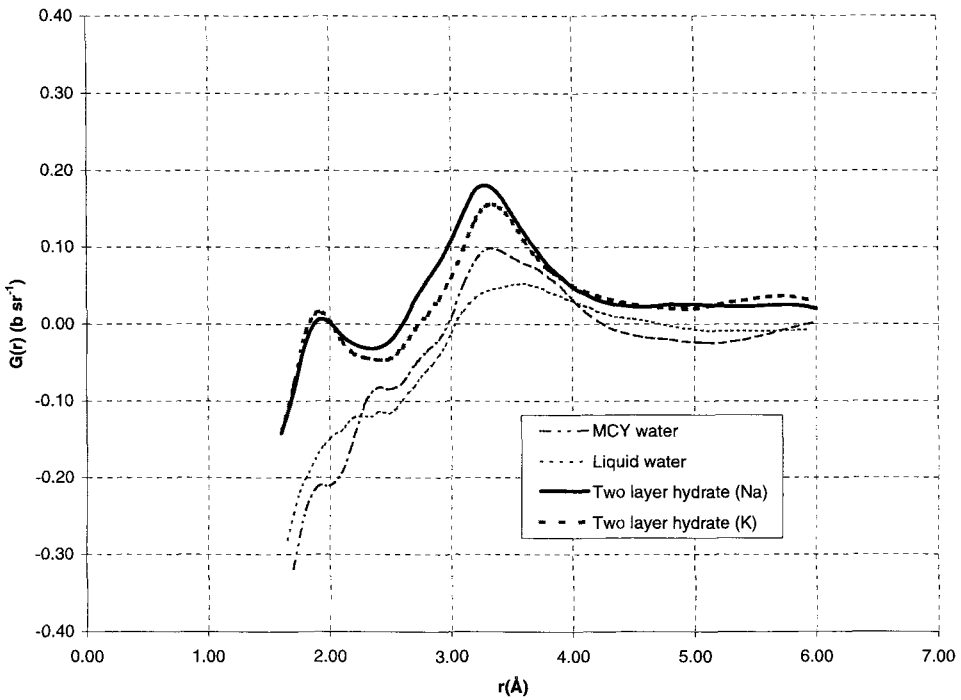

Figure 5. Graph of $G(r)$ for interlayer water in the two-layer hydrate of Na- or K-montmorillonite (simulated), for MCY water (simulated) and for liquid water (experimental).

departure from local tetrahedral ordering among interlayer water molecules, which often have several oxygen ions in the clay mineral surface along with water oxygen atoms as nearest neighbors within a sphere of radius 4 Å. By contrast, a water molecule in the bulk liquid is typically surrounded by four to five nearest neighbors within a smaller sphere of radius 3.5 Å [cf. Figures 21 and 22 in Beveridge *et al.* (1983)]. In their MC simulations of ionic solutions based on the MCY model, Mezei and Beveridge (1981) observed that this local tetrahedral coordination environment was re-established for water molecules outside the octahedral solvation shells of Na^+ and K^+. For interlayer water, however, the clay mineral surface intervenes. Table 2 quantifies these considerations by demonstrating the greater number of nearest-neighbor O (N_{OO}) and the smaller number of hydrogen bonds per O (N_{OH}) in interlayer water as compared to bulk liquid water.

Differences in $g_{OO}(r)$ between Figures 3 and 4 indicate that interlayer water is less well organized in the K-montmorillonite hydrate than in the Na-montmorillonite hydrate. For K-montmorillonite (Figure 4), following the first peak in $g_{OO}(r)$ there is scarcely a minimum, the depth of which is known to be greater as the degree of local tetrahedral coordination among water molecules increases (Kusalik and Svishchev, 1994). [Note also that this minimum is deeper in liquid water (Figure 2) than in MCY water (Figure 1).] Therefore, interlayer water in K-montmorillonite, more so than in Na-montmorillonite, does not mimic well the local coordination structure in bulk liquid water. This situation is likely an effect of the weak solvation of K^+ (Ohtaki and Radnai, 1993), which permits the clay-mineral surface to have greater influence on the structure of interlayer water. Consistently with this hypothesis, Mezei and Beveridge (1981) observed no direct effect of K^+ solvation on the bulk water structure in their MCY-model MC simulations of ionic solutions.

Total radial distribution functions

Figure 5 shows total radial distribution functions based on Equation (6) or (7) and the appropriate RDFs in Figures 1 to 4. The differences between $G_w(r)$ for MCY water and liquid water occur mainly from the relatively large weight given in Equation (7) to $g_{HH}(r)$, which is the RDF least well-predicted by the MCY model (cf. Figures 1 and 2; column 5 in Table 2). A similar discrepancy exists for the second peak in $g_{OH}(r)$, producing in the MCY prediction of $G_w(r)$ near $r \approx 3.4$ Å, a palpable difference from the value for liquid water. It is noteworthy in this context that $g_{OO}(r)$ contributes little to $G_w(r)$ because of its small weight in Equation (7).

The values of $G_h(r)$ predicted for the two montmorillonite hydrates in Figure 5 lie above those of $G_w(r)$, a feature that can be attributed to the larger amplitudes of the two principal contributing RDFs. Powell *et al.* (1997) calculated a hypothetical $G_w(r)$ based on the c and b coefficients that normally would be used for

https://doi.org/10.1346/CCMN.1999.0470209 Published online by Cambridge University Press

$G_h(r)$. Thus, they artificially included clay-mineral structural O and H, instead of using coefficients pertaining only to liquid water (Table 1), with the result that $G_h(r)$ and their hypothetical $G_w(r)$ showed relatively few differences. In the present study, deviations between $G_h(r)$ and $G_w(r)$ do occur because of spatial correlations with the clay mineral structure O and H that do not, of course, exist in bulk liquid water.

The shape of the simulated $G_h(r)$ for either montmorillonite hydrate is similar to that of $G_h(r)$ measured by Powell *et al.* (1997; Figure 5). For example, a well defined peak in the simulated $G_h(r)$ is predicted near $r \approx 1.9$ Å, reflecting O-H spatial correlations, and this peak appears as well in the measured $G_h(r)$, as does the peak predicted to arise near $r \approx 3.3$ Å. Near $r \approx 2.5$ Å, however, the measured distribution function shows a shoulder feature like that in $G_w(r)$, whereas the simulated distribution function does not. Alternatively, the experimental $G_h(r)$ must be a convolution of spatial correlations for interlayer water with those for water adsorbed on external surfaces and in micropores. These latter two types of adsorbed water, which are more likely to be similar to the bulk liquid in structure, were not considered in our MC simulations. Overall, comparing the shapes of $G_h(r)$ and $G_w(r)$ in Figure 5, we conclude, in agreement with Powell *et al.* (1997), that important differences in structure between adsorbed interlayer water and bulk-liquid water should exist over the range of r between 1.5–3.0 Å.

ACKNOWLEDGMENTS

The research reported in this paper was supported in part by the Director, Office of Energy Research, Office of Basic Energy Sciences, Geosciences Division, of the U.S. Department of Energy under contract DE-AC03-76SF00098. The authors thank A. Soper for making available his revised RDF data for liquid water and, along with N. Skipper, J. Greathouse and two anonymous referees, for providing helpful comments on the paper while in draft form. The National Energy Research Scientific Computing Center provided generous allocations of CPU time on its Cray J90 supercomputers. The first author also expresses gratitude to S. M. Benson, Earth Sciences Division, Lawrence Berkeley National Laboratory, for unfailing support, and to A. Zabel for excellent preparation of the typescript.

REFERENCES

Allen, M.P. and Tildesley, D.J. (1987) *Computer simulation of liquids.* Clarendon Press, Oxford 156–159.

Bérend, I., Cases, J-M., François, M., Uriot, J-P., Michot, L., Masion, A., and Thomas, F. (1995) Mechanisms of adsorption and desorption of water vapor by homoionic montmorillonites: 2. The Li^+, Na^+, K^+, Rb^+, and Cs^+-exchanged forms. *Clays and Clay Minerals,* **43,** 324–336.

Beveridge, D.L., Mezei, M., Mehrotra, P.K., Marchese, F.T., Ravi-shanker, G., Vasu, T., and Swaminathan, S. (1983) Monte Carlo computer simulation studies of the equilibrium properties and structure of liquid water. In *Molecular-Based Study of Fluids,* J.M. Haile and G.A. Mansoori, eds., American Chemical Society, Washington, 297–351.

Boek, E.S., Coveney, P.V., and Skipper, N.T. (1995a) Molecular modeling of clay hydration: A study of hysteresis loops in the swelling curves of sodium montmorillonite. *Langmuir,* **11,** 4629–4631.

Boek, E.S., Coveney, P.V., and Skipper, N.T. (1995b) Monte Carlo molecular modeling studies of hydrated Li-, Na-, and K-smectites. Understanding the role of potassium as a clay swelling inhibitor. *Journal of the American Chemical Society,* **117,** 12608–12617.

Calvet, R. (1972) Adsorption de l'eau sur les argiles: Etude de l'hydratation de la montmorillonite. *Bulletin de la Societé Chimique de France 1972,* **8,** 3097–3104.

Cebula, D.J., Thomas, R.K., and White, J.W. (1980) Small angle neutron scattering from dilute aqueous dispersions of clay. *Journal of the Chemical Society, Faraday Transactions I,* **76,** 314–321.

Chang, F-R.C., Skipper, N.T., and Sposito, G. (1995) Computer simulation of interlayer molecular structure in sodium montmorillonite hydrates. *Langmuir,* **11,** 2734–2741.

Chang, F-R.C., Skipper, N.T., and Sposito, G. (1997) Monte Carlo and molecular dynamics simulations of interfacial structure in lithium-montmorillonite hydrates. *Langmuir,* **13,** 2074–2082.

Chang, F-R.C., Skipper, N.T., and Sposito, G. (1998) Monte Carlo and molecular dynamics simulations of electrical double-layer structure in potassium-montmorillonite hydrates. *Langmuir,* **14,** 1201–1207.

Enderby, J.E. (1983) Neutron scattering from ionic solutions. *Annual Review of Physical Chemistry,* **34,** 155–185.

Enderby, J.E. and Neilson, G.W. (1981) The structure of electrolyte solutions. *Reports on Progress in Physics,* **44,** 593–653.

Fu, M.H., Zhang, Z.Z., and Low, P.F. (1990) Changes in the properties of a montmorillonite-water system during the adsorption and desorption of water. Hysteresis. *Clays and Clay Minerals,* **38,** 485–492.

Hawkins, R.K. and Egelstaff, P.A. (1980) Interfacial water structure in montmorillonite from neutron diffraction experiments. *Clays and Clay Minerals,* **28,** 19–28.

Karaborni, S., Smit, B., Heidug, W., Urai, J., and van Oort, E. (1996) The swelling of clays: Molecular simulations of the hydration of montmorillonite. *Science,* **271,** 1102–1104.

Kusalik, P.G. and Svishchev, I.M. (1994) The spatial structure in liquid water. *Science,* **265,** 1219–1221.

Matsuoka, O., Clementi, E., and Yoshimine, M. (1976) CI study of the water dimer potential surface. *Journal of Chemical Physics,* **64,** 1351–1361.

Mezei, M. and Beveridge, D.L. (1981) Monte Carlo studies of the structure of dilute aqueous solutions of Li^+, Na^+, K^+, F^-, and Cl^-. *Journal of Chemical Physics* **74,** 6902–6910.

Neilson, G.W. and Enderby, J.E. (1989) The coordination of metal ions. *Advances in Inorganic Chemistry,* **34,** 195–217.

Ohtaki, H. and Radnai, T. (1993) Structure and dynamics of hydrated ions. *Chemical Reviews,* **93,** 1157–1204.

Posner A.M. and Quirk, J.P. (1964) Changes in basal spacing of montmorillonite in electrolyte solutions. *Journal of Colloid Science,* **19,** 798–812.

Powell, D.H., Tongkhao, K., Kennedy, S.J., and Slade, P.G. (1997) A neutron diffraction study of interlayer water in sodium Wyoming montmorillonite using a novel difference method. *Clays and Clay Minerals,* **45,** 290–294.

Skipper, N.T. and Neilson, G.W. (1989) X-ray and neutron diffraction studies on concentrated aqueous solutions of sodium nitrate and silver nitrate. *Journal of Physics: Condensed Matter,* **1,** 4141–4154.

Skipper, N.T., Soper, A.K., and McConnell, J.D.C. (1991) The structure of interlayer water in vermiculite. *Journal of Chemical Physics,* **94,** 5751–5760.

Skipper, N.T., Soper, A.K., and Smalley, M.V. (1994) Neutron diffraction study of calcium vermiculite: Hydration of cal-

cium ions in a confined environment. *Journal of Physical Chemistry,* **98,** 942–945.

Skipper, N.T., Chang, F.R., and Sposito, G. (1995a) Monte Carlo simulation of interlayer molecular structure in swelling clay minerals. 1. Methodology. *Clays and Clay Minerals,* **43,** 285–293.

Skipper, N.T., Sposito, G., and Chang, F.R. (1995b) Monte Carlo simulation of interlayer molecular structure in swelling clay minerals. 2. Monolayer hydrates. *Clays and Clay Minerals,* **43,** 294–303.

Skipper, N.T., Smalley, M.V., Williams, G.D., Soper, A.K., and Thompson, C.H. (1995c) Direct measurement of the electrical double-layer structure in hydrated lithium vermiculite clays by neutron diffraction. *Journal of Physical Chemistry,* **99,** 14201–14204.

Slade, P.G., Quirk, J.P., and Norrish, K. (1991) Crystalline swelling of smectite samples in concentrated NaCl solutions in relation to layer charge. *Clays and Clay Minerals,* **39,** 234–238.

Soper, A.K. and Phillips, M.G. (1986) A new determination of the structure of water at 25°C. *Chemical Physics,* **107,** 47–60.

Soper, A.K., Bruni, F., and Ricci, M.A. (1997) Site-site pair correlation functions of water from 25 to 400°C: Revised analysis of new and old diffraction data. *Journal of Chemical Physics,* **106,** 247–254.

Zhang, Z.Z. and Low, P.F. (1989) Relation between the heat of immersion and the initial water content of Li-, Na-, and K-montmorillonite. *Journal of Colloid Interface Science,* **133,** 461–472.

(Received 30 March 1998; accepted 15 September 1998; Ms. 98-039)